ELSEVIER

Journal of Organometallic Chemistry 579 (1999) 5–17

Journal of Organometallic Chemistry

Derivative chemistry of $[UCl_2\{B(pz)_4\}_2]$: stability of complexes containing the fragments $[U\{B(pz)_4\}_2]$ and $[U\{HB(pz)_3\}_2]$

M. Paula C. Campello [a], Ângela Domingos [a], Adelino Galvão [b], A. Pires de Matos [a], Isabel Santos [a,*]

[a] *Departamento de Química, ITN, P-2686 Sacavém Codex, Portugal*
[b] *Departamento de Engenharia Química, Instituto Superior Técnico, P-1096 Lisboa Codex, Portugal*

Received 22 July 1998; received in revised form 18 November 1998

Abstract

Uranium tetrachloride reacts with two equivalents of $K[B(pz)_4]$ in THF affording $[UCl_2\{B(pz)_4\}_2]$ (**1**) in 75% yield. Complex **1** is monomeric and crystallizes in the monoclinic space group $C2/c$ with cell parameters $a = 13.700(6)$, $b = 12.759(2)$, $c = 17.513(8)$ Å, $\beta = 101.37(2)°$, $V = 3001(2)$ Å^3, $Z = 4$. Derivatives $[UCl(OR)\{B(pz)_4\}_2]$ (R = C_2H_5 (**2**), ^{t}Bu (**3**), C_6H_4-*o*-OMe (**4**) and C_6H_2-2,4,6-Me_3 (**5**)), $[U(O^tBu)_2\{B(pz)_4\}_2]$ (**6**), $[U(S^iPr)_2\{B(pz)_4\}_2]$ (**7**) and $[UCl(Me)\{B(pz)_4\}_2]$ (**8**) were obtained by reacting **1** with sodium alkoxides, with NaS^iPr or with LiMe. X-ray crystallographic analysis of **5** and **7** shows that uranium is eight-coordinate by the two η^3-$[B(pz)_4]$ ligands and by two monodentate coligands (**5**: crystallizes in the monoclinic space group $C2/c$ with cell parameters $a = 30.575(3)$, $b = 9.929(1)$, $c = 24.884(3)$ Å, $\beta = 90.59(1)°$, $V = 7554(1)$ Å^3, $Z = 8$; **7** crystallizes in the monoclinic space group $C2/c$ with cell parameters $a = 24.286(7)$, $b = 9.471(2)$, $c = 16.076(3)$ Å, $\beta = 96.44(3)°$, $V = 3674(2)$ Å^3, $Z = 4$). Extended Hückel molecular orbital (EHMO) calculations were used to get a better insight into the electronic properties of the ligand $[B(pz)_4]$ and to get some explanation on the relative stability of complexes containing the fragments '$[U\{B(pz)_4\}_2]$' and '$[U\{HB(pz)_3\}_2]$'.

Keywords: Uranium; Poly(pyrazolyl)borates; EHMO calculations; Stability

1. Introduction

The steric and electronic properties of the poly(pyrazolyl)borates are greatly affected by the number and nature of the groups bonded to the boron atom and also by the type of pyrazolyl substituents [1,2]. These properties are responsible for the type of complexes stabilized with *d*- and *f*-elements and play a dominant role in determining the coordination number, the geometry, and the behaviour of the complexes in solution. With *f*-elements, the compounds $[UCl_2\{HB(pz)_3\}_2]$ and $[UCl_3\{HB(3,5\text{-}Me_2pz)_3\}]$ are clearly an example of how the substituents affect the structure, solution behaviour and derivative chemistry [3].

With the $[HB(pz)_3]^-$ and $[B(pz)_4]^-$ ligands some chemistry has been done, especially with *d*-transition elements, but structure, stability and reactivity of analogous complexes have not been systematically compared [1,2,4]. Only recently, Sohrin et al. published a systematic study with these ligands and with Group 2 elements, comparing stabilities and analyzing intra and interligand contacts by molecular mechanics calculations [5,6].

As part of our ongoing work on uranium chemistry, we decided to compare the chemistry of the ancillary ligands $[HB(pz)_3]^-$ and $[B(pz)_4]^-$. Here we report the structural characterization of $[UCl_2\{B(pz)_4\}_2]$ (**1**) and the use of this complex as a precursor for the synthesis of compounds containing oxygen, sulfur, nitrogen and carbon donor coligands. Extended Hückel molecular orbital (EHMO) calculations have been

* Corresponding author. Tel.: +351-1-955-0021; fax: +351-1-994-1455.
E-mail address: isantos@itn1.itn.pt (I. Santos)

0022-328X/99/$ - see front matter
PII: S0022-328X(98)01134-6

performed to get a better insight into the differences found in complexes with the moieties $[U\{B(pz)_4\}_2]$ and $[U\{HB(pz)_3\}_2]$.

2. Experimental

2.1. General procedures

All reactions were carried out under argon, using standard Schlenk and vacuum-line techniques or in an argon-filled glove-box. Solvents were dried and deoxygenated by standard methods [7] and distilled immediately prior to use. $CDCl_3$ was dried over P_2O_5 and C_6D_6 was dried over Na/benzophenone. Acetone was dried with $CaSO_4$ and then distilled from $CaSO_4$. UCl_4 and $K[B(pz)_4]$ were prepared by published methods [4,8]. $NaOC_2H_5$, $NaOCMe_3$ and $NaOC_6H_2$-2,4,6Me_3 were prepared by reacting Na with the respective alcohols. KOC_6H_4-*o*-OMe was prepared by reacting KH with HOC_6H_4-*o*-OMe. $LiCH_3$ (Aldrich) was used without further purification. $KCH_2C_6H_5$, $LiCH_2SiMe_3$ and Li-CH_2CMe_3 were prepared by published methods [9–11].

^{1}H-NMR spectra were recorded on a Varian 300 MHz multinuclear spectrometer, using the chemical shift of the solvent as the internal standard. IR spectra were recorded as Nujol mulls on a Perkin–Elmer 577 spectrophotometer. Absorption electronic spectra were recorded as solutions on a Cary 2390 Varian spectrometer. Carbon, hydrogen and nitrogen analyses were performed on a Perkin–Elmer automatic analyser.

2.2. Synthesis and characterization of $[UCl_2\{B(pz)_4\}_2]$ (1)

To a solution of UCl_4 (250 mg, 0.66 mmol) in THF (20 cm^3) $K[B(pz)_4]$ (419 mg, 1.32 mmol) was slowly added. After overnight reaction, at room temperature (r.t.), the reaction mixture was centrifuged and the green solution was taken to dryness, yielding a green solid which was washed with *n*-hexane. Complex **1** presents a limited solubility in THF and a significant amount precipitates with KCl. This fraction is recovered by extraction with dichloromethylene (434 mg, 0.50 mmol, 75% yield).

Anal. Found: C, 33.7%; H, 2.8%; N, 25.6%. $C_{24}H_{24}B_2Cl_2N_{16}U$ Calc.: C, 33.2%; H, 2.8%; N, 25.8%. IR (Nujol, ν(cm^{-1})): 3130(m), 3105(m), 3090(m), 1497(s), 1486(s), 1409(s), 1385(s), 1289(s), 1252(w), 1220(s), 1210(s), 1188(s), 1097(s), 1080(s), 1074(s), 975(w), 957(w), 922(m), 885(m), 879(w), 848(s), 832(s), 786(s), 776(s), 749(s), 688(m), 677(m), 630(m), 351(s), 335(m), 332(w), 320(w), 300(w), 280(w), 253(m), 239(m), 221(m). UV–vis. (CH_2Cl_2 or THF) (λ_{max}(nm)): 450(w), 500(m), 570(m), 670(s), 690(vs), 860(vw), 1080(s), 1120(s), 1180(s), 1620(m).

2.3. Synthesis and characterization of $[UCl(OC_2H_5)\{B(pz)_4\}_2]$ (2)

To a suspension of **1** (215 mg, 0.25 mmol) in toluene (10 cm^3) was added $NaOC_2H_5$ (17 mg, 0.25 mmol). After overnight reaction, the bright green solution was separated by centrifugation and evaporated to dryness, yielding a green crystalline solid (172 mg, 0.20 mmol, 79% yield).

Anal. Found: C, 35.2%; H, 3.2%; N, 25.1%. $C_{26}H_{29}B_2ClN_{16}OU$ Calc.: C, 35.6%; H, 3.3%; N 25.6%. IR (Nujol, ν(cm^{-1})): 3147(m) 3138(m), 1730(w), 1616(vw), 1501(s), 1466(s), 1435(s), 1400(s), 1380(s), 1286(s), 1260(m), 1230(m), 1200(s), 1112(s), 1060(s), 975(s), 956(m), 917(s), 864(m), 847(s), 811(s), 755(s), 676(m), 659(m), 617(s), 499(m), 386(m), 358(m), 337(m), 277(m), 269(s), 246(m), 223(m), 209(m). UV–vis. (Toluene) (λ_{max}(nm)): 620(m), 730(w), 970(m), 1050(vs), 1120(m), 1270(m), 1380(s), 1410(s), 1510(s).

2.4. Synthesis and characterization of $[UCl(O^tBu)\{B(pz)_4\}_2]$ (3)

2.4.1. Method 1

Compound **3** was obtained as described above for **2** (250 mg, 0.29 mmol, of **1** in 10 cm^3 toluene and 28 mg, 0.29 mmol, of $NaOCMe_3$). Compound **3** was obtained as a green complex in 66% yield (173 mg, 0.19 mmol).

2.4.2. Method 2

To a suspension of **1** (182 mg, 0.21 mmol) in toluene (10 cm^3) were added O=CMe_2 (12 mg, 0,21 mmol) and a solution of MeLi (5% in diethylether) (108 mg, 0.21 mmol). After 1 h, the green solution was separated by centrifugation and evaporated to dryness. The obtained bright green solid was washed with *n*-hexane and dried in vacuo (144.8 mg, 0.16 mmol, yield 75%).

Anal. Found: C, 38.2%; H, 3.4%; N, 23.4%. $C_{28}H_{33}B_2ClN_{16}OU$ Calc.: C, 37.2%; H, 3.7%; N, 24.8%. IR (Nujol, ν(cm^{-1})): 3125(m), 1743(m), 1647(w), 1499(s), 1466(m), 1435(m), 1400(m), 1381(m), 1365(m), 1307(w), 1280(s), 1255(m), 1233(m), 1210(s), 1193(w), 1110(s), 1080(m), 1070(m), 1045(m), 1026(w), 944(s), 922(s), 895(w), 864(m), 848(s), 815(m), 796(s), 777(m), 763(s), 724(m), 695(w), 676(m), 618(s), 525(s), 493(m), 473(m), 356(s), 339(m), 257(m), 241(s). UV–vis: (toluene) (λ_{max}(nm)): 650(w), 965(m) 1045(s), 1080(s), 1120(sh, w), 1265(m), 1380(m), 1490(m).

^{1}H-NMR in toluene-d_8 at 180 K (δ(ppm)): 297.0 (1H), 121.1 (1H), 116.6 (9H, O^{t}Bu), 60.5 (2H), 50.9 (1H), 42.6 (1H), 17.1 (1H), 7.5 (1H), 4.6 (1H), 1.8 (1H),

0.5 (1H), −3.2 (1H), −7.1 (1H), −15.7 (2H), −20.9 (1H), −22.4 (2H), −24.4 (1H), −26.0 (1H), −31.0 (2H), −87.6 (1H), −102.1 (1H).

^{1}H-NMR in toluene-d_8 at 340 K (δ (ppm)): 61.3 (9H, O^{t}Bu), 24.6 (8H, [B(pz)$_4$]), 6.2 (8H, [B(pz)$_4$]), 1.4 (8H, [B(pz)$_4$]).

2.5. Synthesis and characterization of [UCl(OC$_6$H$_4$-*o*-OCH$_3$){B(pz)$_4$}$_2$] (4)

Compound **1** (150 mg, 0.17 mmol) in toluene (10 cm^3) reacts with KOC$_6$H$_4$-*o*-OCH$_3$ (28 mg, 0,17 mmol) yielding a green crystalline solid which was formulated as **4**, after work-up (117 mg, yield 72%).

Anal. Found: C, 40.8%; H, 3.1%; N, 22.0%. $C_{31}H_{31}B_2ClN_{16}O_2U$ Calc.: C, 39.0%; H, 3.3%; N, 23.5%. IR (Nujol, ν(cm^{-1})): 3134(m), 1752(w), 1582(m), 1497(s), 1432(s), 1402 (s), 1379(s), 1300(s), 1287(s), 1262(s), 1205(s), 1184(m), 1107(s), 1090(s), 1063(s), 1042(w), 1023(m), 982(m), 963(w), 918(m), 877(w), 865(m), 848(s), 803(s), 762(s), 695(m), 670(m), 658(m), 616(s), 551(w), 466(w), 398(w), 359(w), 281(w), 249(m), 244(w), 214(w). UV–vis (toluene) (λ_{max}(nm)): 660(f), 710(w), 1080(sh, m), 1090(sh, m), 1110(sh, m), 1370(m), 1470(m).

2.6. Synthesis and characterization of [UCl(OC$_6$H$_2$-2,4,6-Me$_3$){B(pz)$_4$}$_2$] (5)

Compound **1** (200 mg, 0.23 mmol) in toluene (10 cm^3) reacts with NaOC$_6$H$_2$-2,4,6Me$_3$ (36 mg, 0.23 mmol). After overnight reaction, the bright green solution was separated by centrifugation and evaporated to dryness, yielding a green crystalline solid formulated as **5** (138 mg, 0.14 mmol, yield 62%).

Anal. Found: C, 40.2%; H, 3.8%; N, 22.1%. $C_{33}H_{35}B_2ClN_{16}OU$ Calc.: C, 40.9%; H, 3.7%; N, 23.2%. IR (Nujol, ν(cm^{-1})): 3140(m), 3130(m), 1730(w), 1504(s), 1468(s), 1434(s), 1375(s), 1290(s), 1259(w), 1230(s), 1198(s), 1150(s), 1102(s), 1087(m), 1059(s), 981(m), 956(w), 917(m), 894(vw), 847(s), 802(s), 755(s), 725(m), 671(m), 656(m), 615(s), 588(w), 571(w), 554(m), 386(w), 361(m), 345(m), 315(m), 249(s), 238(s). UV–vis (toluene) (λ_{max}(nm)): 660(m), 780(w), 990(m), 1090(vs), 1140(m), 1335(m), 1470(m).

^{1}H-NMR in toluene-d_8 at 180 K (δ (ppm)): 219.0 (1H), 195.3 (1H), 86.5 (1H), 72.2 (1H), 69.4 (3H, *o*-Me), 62.8 (1H, *m*-H + 1H), 59.4 (1H, *m*-H), 55.4 (1H), 48.0 (1H), 46.3 (3H, *o*-Me), 37.3 (3H, *p*-Me), 36.2 (1H), 18.7 (1H), 3.0 (1H), −0.8 (1H), −4.0 (1H), −8.7 (2H), −13.9 (2H), −21.6 (1H), −23.7 (1H), −28.7 (2H), −29.3 (1H), −31.2 (1H), −131.4 (1H), −147.7 (1H).

^{1}H-NMR in toluene-d_8 at 360 K (δ (ppm)): 32.8 (2H, *m*-H), 27.9 (8H, [B(pz)$_4$]), 25.3 (6H, *o*-Me), 18.9 (3H, *p*-Me), 5.4 (8H, [B(pz)$_4$]), 0.9 (8H, [B(pz)$_4$]).

2.7. Synthesis and characterization of [U{O^{t}Bu}$_2${B(pz)$_4$}$_2$] (6)

NaO^{t}Bu (67 mg, 0.68 mmol) reacts with **1** (300 mg, 0.34 mmol) in toluene (10 cm^3). After overnight reaction, the dark green solution was separated by centrifugation and evaporated to dryness, yielding a green crystalline solid. Several attempts have been made to get single crystals, however **6** decomposes in solution affording uncharacterizable brown solids.

Anal. Found: C, 38.5%; H, 4.5%; N, 22.8%. $C_{32}H_{42}B_2N_{16}O_2U$ Calc: C, 40.8%; H, 4.5%; N, 23.8%. IR (Nujol, ν(cm^{-1})): 3150(w), 3139(w), 1745(w), 1605(w), 1502(s), 1459(m), 1432(m), 1405(s), 1382(s), 1357(m), 1295(s), 1260(m), 1213(w), 1190(s), 1099(s), 1083(w), 1065(s), 1024(w), 974(s), 922(m), 892(w), 863(w), 847(s), 811(s), 759(s), 729(s), 695(m), 674(m), 658(w), 620(m), 504(m), 481(m), 462(m), 398(m), 358(m), 247(m), 238(m), 231(m), 217(m). UV–vis (toluene) (λ_{max}(nm)): 665(w), 985(m), 1035(s), 1105(s), 1270(m), 1405(m).

^{1}H-NMR in toluene-d_8 at 190 K (δ, ppm): 76.92 (2H), 43.7 (2H), 22.7 (2H), 18.7 (18H, O^{t}Bu), 14.0 (2H), 7.6 (2H), 3.9 (2H), 1.8 (2H), 0.1 (2H), −9.7 (2H), −11.1 (2H), −11.4 (2H), −23.0 (2H).

^{1}H-NMR in toluene-d_8 at 340 K (δ (ppm)): 17.8 (8H, [B(pz)$_4$]), 13.6 (18H, O^{t}Bu), 5.3 (8H, [B(pz)$_4$]), 2.0 (8H, [B(pz)$_4$]).

2.8. Synthesis and characterization of [U{S^{i}Pr}$_2${B(pz)$_4$}$_2$] (7)

To a suspension of **1** (450 mg, 0.52 mmol) in toluene (15 cm^3) NaS^{i}Pr was added (103 mg, 1.04 mmol). After overnight reaction, the orange solution was separated by centrifugation and evaporated to dryness. The obtained orange solid was washed with *n*-hexane and dried (400 mg, 0.42 mmol, yield 80%).

Anal. Found: C, 37.9%; H, 3.8%; N, 22.9%. $C_{30}H_{38}B_2N_{16}S_2U$ Calc: C, 39.6%; H, 3.9%; N, 23.1%. IR (Nujol, ν(cm^{-1})): 3100(w), 1502(s), 1450(m), 1380(m), 1360(s), 1280(s), 1250(w), 1210(w), 1190(s), 1175(s), 1140(w), 1090(s), 1060(w), 1050(m) 1040(m), 980(m), 960(w), 860(w), 840(s), 800(s), 760(s), 660(w), 610(m), 360(m). UV–vis (toluene) (λ_{max}(nm)): 580(w), 600(w), 1058(s), 1410(br, m).

^{1}H-NMR in toluene-d_8 at 190 K (δ (ppm)): 76.0 (2H), 62.8 (2H), 22.2 (6H, CH$_3$, S^{i}Pr), 19.5 (2H), 17.5 (6H, CH$_3$, S^{i}Pr), 17.4 (2H, CH, S^{i}Pr), 16.6 (2H), 8.7 (2H), 5.9 (2H), 3.2 (2H free), −1.3 (2H, free), −12.9 (2H, free), −13.1 (2H), 14.3 (2H), −20.8 (2H).

2.9. Synthesis and characterization of [UCl(Me){B(pz)$_4$)}$_2$] (8)

To a suspension of **1** (180 mg, 0.21 mmol) in toluene (25 cm^3) was added LiMe (109 mg, 0.21 mmol) in

toluene (20 cm^3). The reaction was allowed to react during 2 h, centrifuged and the supernatant was vacuum dried and washed with *n*-hexane (72 mg, 0.08 mmol, 42%).

Anal. Found: C, 36.5%; H, 2.5%; N, 26.5%. $C_{25}H_{27}B_2N_{16}ClU$ Calc: C, 35.5%; H, 3.2%; N, 26.5%. IR (Nujol, $\nu(cm^{-1})$): 3134(w), 2360(w), 1504(s), 1460(s), 1400(s), 1378(s), 1297(s), 1287(s), 1261(s), 1211(s), 1193(s), 1108(s), 1094(s), 1062(s), 1020(m), 980(s), 965(s), 922(m), 893(s), 863(s), 847(m), 832(s), 811(s), 777(w), 760(w), 727(m), 670(w), 616(m), 466(m), 397(m), 277(m), 251(m). UV–vis (toluene) (λ_{max}(nm)): 620(w), 845 (w), 1000(s), 1048(s), 1110(m), 1310(w).

2.10. X-ray crystallographic analysis

X-ray data were collected from a green crystal of **1** obtained by recrystallization from dichloromethane/*n*-hexane, from a green crystal of **5** and from an orange crystal of **7** obtained by slow diffusion of *n*-hexane into a saturated solution of the complexes in toluene. The crystals were mounted in thin-walled glass capillaries within a nitrogen filled glove-box.

Data were collected at r.t. on an Enraf–Nonius CAD-4 diffractometer with graphite-monochromatized Mo–K_α radiation, using a ω–2θ scan mode. Unit cell dimensions were obtained by least-squares refinement of the setting angles of 25 reflections with $20.0 < 2\theta < 32.0°$ for **1**, $16.9 < 2\theta < 31.6°$ for **5** and $16.0 < 2\theta < 27.4°$ for **7**. The crystal data are summarized in Table 1. The data were corrected [12] for Lorentz and polarization effects, for linear decay and also for absorption (ψ-scans). The heavy atom positions were located by Patterson methods using SHELXS-86 [13], being at special positions in **1** and **7**, on a 2-fold rotation axis. The remaining atoms were located by successive difference Fourier techniques and refined by full-matrix least-squares on *F* using SHELX-76 for **1**, and on F^2 with SHELXL-93 for **5** and **7** [14]. All the non-hydrogen atoms were refined with anisotropic thermal motion parameters. The contributions of the hydrogen atoms were included in idealized positions. The final difference Fourier syntheses revealed electron densities between $+3.24$ and -2.81 e $Å^{-3}$ for **1** and 0.83 and -0.92 e $Å^{-3}$ for **5**, near the uranium atom. For **7**, some residual electron densities were found near the uranium atom between $+5.41$ and -1.25 e $Å^{-3}$, the strongest peak being 1.66 and 1.96 Å from the uranium and sulfur atoms on the 2-fold rotation axis. Atomic scattering factors and anomalous dispersion terms were taken from the International Tables for X-ray Crystallography [15]. The drawings were made with ORTEPII. [16].

3. Results and discussion

Uranium tetrachloride reacts with two equivalents of $K[B(pz)_4]$ in THF at r.t. to afford the complex $[UCl_2\{B(pz)_4\}_2]$ (**1**) in 75% yield [17]. This complex is very stable either in solid or in solution, presents a high solubility in chlorinated solvents and is moderately soluble in THF.

Table 1
Crystallographic data for **1**, **5**, and **7**

Compound	**1**	**5**	**7**
Empirical formula	$C_{24}H_{24}B_2N_{16}Cl_2U$	$C_{33}H_{35}B_2N_{16}ClOU$	$C_{30}H_{38}B_2N_{16}S_2U$
Formula weight	867.12	966.87	946.53
Crystal system	Monoclinic	Monoclinic	Monoclinic
Space group	*C*2/*c*	*C*2/*c*	*C*2/*c*
a (Å)	13.700(6)	30.575(3)	24.286(7)
b (Å)	12.759(2)	9.929(1)	9.471(2)
c (Å)	17.513(8)	24.884(3)	16.076(3)
β (°)	101.37(2)	90.59(1)	96.44(3)
V ($Å^3$)	3001(2)	7554(1)	3674(2)
Z	4	8	4
$D_{calc.}$ (g cm^{-3})	1.919	1.700	1.711
Absorption coefficient (cm^{-1}) (Mo–K_α)	56.34	44.20	45.79
Number of reflections	3189	6588	3231
Number of paramaters refined	206	488	234
Refinement method	*F*	F^2	F^2
R_1[a]	$0.045(F_o > 3\sigma(F_o))$	$0.0282(F_o > 4\sigma(F_o))$	$0.0583(F_o > 4\sigma(F_o))$
R_w[b]	$0.051(F_o > 3\sigma(F_o))$	$0.0544(F_o > 4\sigma(F_o))$	$0.1218(F_o > 4\sigma(F_o))$

[a] $R_1 = \Sigma||F_o|-|F_c||/\Sigma|F_o|$.

[b] For **1**, $R_w = [\Sigma w||F_o|-|F_c||^2/\Sigma w|F_o|^2]^{1/2}$; $w = [\sigma^2(F_o)+g(F_o^2)]^{-1}$ where $g = 0.001$. For **5** and **7**, $R_w = wR_2 = [\Sigma(w(F_o^2-F_c^2)^2)/\Sigma(w(F_o^2)^2)]^{1/2}$; $w = 1/[\sigma^2(F_o^2)+(aP)^2+bP]$, where $P = (F_o^2+2F_c^2)/3$.

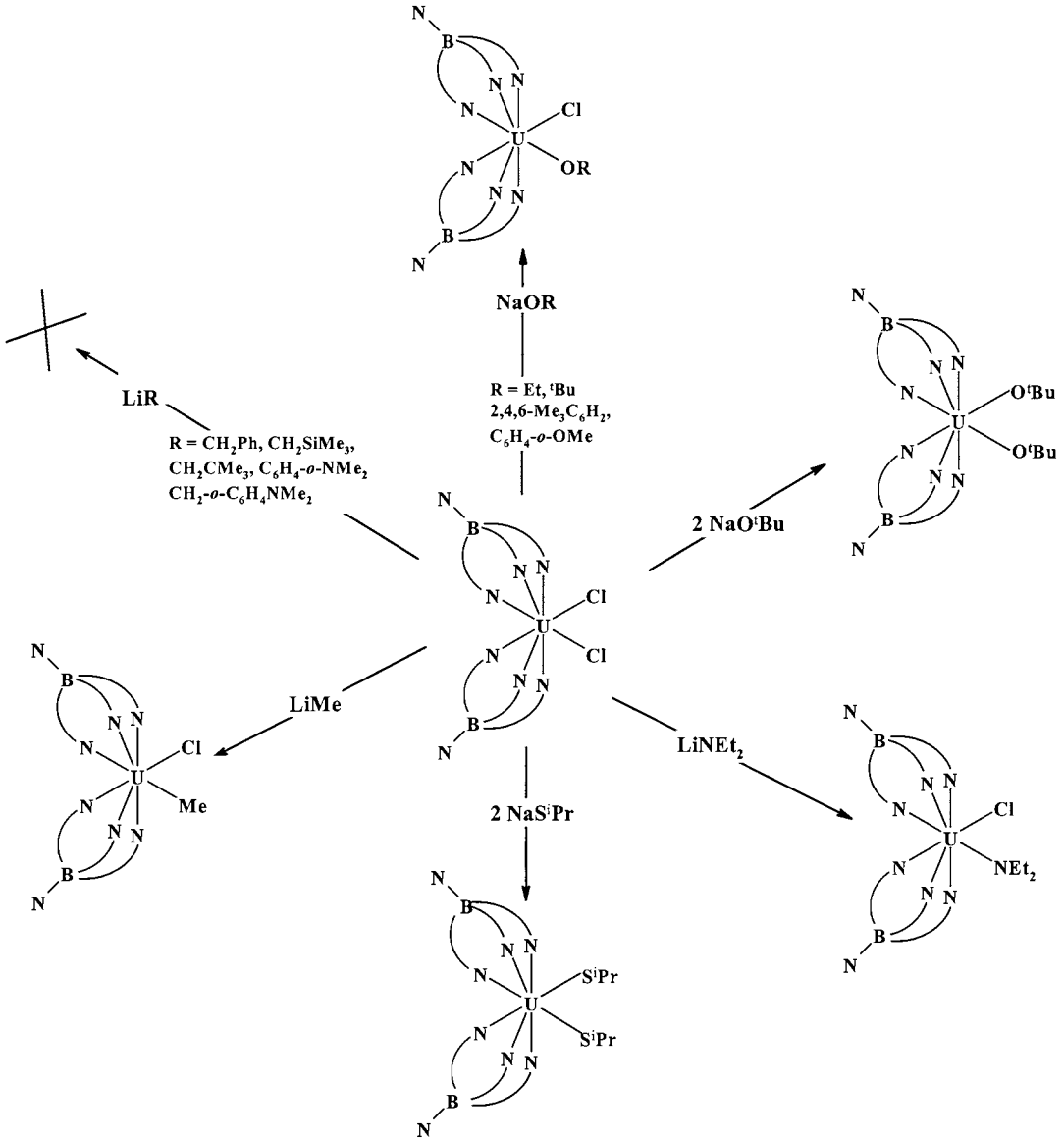

Scheme 1.

$$UCl_4 + 2K[B(pz)_4] \xrightarrow{THF} [UCl_2\{B(pz)_4\}_2] + 2KCl$$

Complex **1** reacts with one equivalent of NaOR ($R = C_2H_5$, ^{t}Bu, C_6H_4-*o*-OMe and C_6H_2-2,4,6-Me_3) in toluene affording the corresponding derivatives $[UCl(OR)\{B(pz)_4\}_2]$ ($R = C_2H_5$ (**2**), ^{t}Bu (**3**), C_6H_4-*o*-OMe (**4**) and C_6H_2-2,4,6-Me_3 (**5**)). Complexes $[U(O^tBu)_2\{B(pz)_4\}_2]$ (**6**) and $[U(S^iPr)_2\{B(pz)_4\}_2]$ (**7**) were also obtained by reacting **1** with two equivalents of NaO^{t}Bu and NaS^{i}Pr, respectively (Scheme 1).

In solution, complexes **1**–**5** are stable even at high temperatures, **6** decomposes slowly at r.t. and **7** decomposes at temperatures higher than 20°C.

The synthesis of derivatives with uranium–nitrogen bonds has also been tried. Complex $[UCl(NEt_2)\{B(pz)_4\}_2]$ although being formed (as indicated by ^{1}H-NMR) decomposes readily in solution and cannot be isolated in a pure form. Several attempts were also made to prepare derivatives with metal–carbon bonds but the only isolated complex in a pure form was $[UCl(Me)\{B(pz)_4\}_2]$ (**8**) (40%, yield) (Scheme 1). In some of the reactions with lithium alkyls the metal centre is reduced to U(III), as shown by the electronic spectra, but we were unable to fully characterise these species [18].

In our hands, the derivative chemistry of **1** is limited, when compared with the chemistry that we have done previously using the starting material $[UCl_2\{HB(pz)_3\}_2]$. With this complex a larger number of derivatives with metal–carbon, metal–nitrogen, metal–sulfur and metal–oxygen bonds were stabilized [19–25].

Complexes **2**–**7** are soluble in THF, aromatic, aliphatic and chlorinated hydrocarbons, while **8** is only soluble in aromatic and aliphatic solvents.

3.1. ^{1}H-NMR spectra

Table 2 displays the ^{1}H-NMR data for **1**–**8**. Compounds **1**–**4**, **7** and **8** present two sets of resonances of relative intensity 1:3 for the H(3), H(4) and H(5) protons of the uncoordinated and coordinated pyrazolyl rings. For **5** only the resonances due to the H(3), H(4) and H(5) protons of the uncoordinated pyrazolyl rings are observed and for **6** no resonances appear for the tetrakis(pyrazolyl)borate ligands. In all compounds (**2**–**8**), the resonances due to the coligands appear at low field, with chemical shifts comparable to those found previously for the analogous complexes with the moiety $[U\{HB(pz)_3\}_2]$ [19–25].

The pattern observed in the ^{1}H-NMR spectra of **1**–**8** for the protons of the tetrakis(pyrazolyl)borate ligands is explained by the fluxional behaviour of these complexes in solution. For **1**–**4**, **7** and **8** an intramolecular and non dissociative dynamic process exists and is fast on the NMR time scale. This process is responsible for the magnetic equivalence of the six-coordinated pyrazolyl rings and for the equivalence of the two uncoordinated rings, remaining coordinated and uncoordinated rings magnetically different. The mechanism involved is certainly the interconversion of the common eight-coordinate polyhedra (square antiprismatic (SAP)⇔dodecahedron (DD)⇔bicapped trigonal prism (BCTP)) [19–25].

For complexes **5** and **6** the rate of the dynamic process is slow on the NMR time scale, just at r.t., and this justifies the absence of some (**5**) or of all (**6**) the resonances due to the tetrakis(pyrazolyl)borate ligands.

Variable temperature ^{1}H-NMR studies for **1**, **2**, **4** and **8** indicate that the chemical shifts of all the resonances follow an approximate Curie relationship, but their line shape is temperature independent. For **3** and **5**–**7**, by lowering the temperature, it was possible to slow down the interconversion of the common eight-coordinate polyhedra (SAP⇔DD⇔BCTP) and static spectra were obtained between 220 and 180 K. The static spectra of **6** and **7** present twelve resonances of equal intensity (Section 2). This pattern indicates the magnetic equivalence of the two tetrakis(pyrazolyl)borate ligands but indicates also that in each ligand all the pyrazolyl rings are different. This pattern agrees with the C_2 symmetry expected for these complexes in the solid state, and confirmed by the X-ray structural analysis of **7** (vide infra). The C_2 symmetry of **7** also justifies the splitting observed for the thiolate ligands: one resonance for the methynic protons and two resonances for the diastereotopic methyl groups.

For compounds **3** and **5** a C_1 symmetry is expected in the solid state (vide X-ray of **5**). As the compounds must adopt at low temperature, a structure analogous to the solid state, we would expect to obtain static spectra with 24 resonances. In fact, due to the freezing point of the solvent, we were not able to go below 180 K and at this temperature we only observed 20 resonances, due to the occasional overlapping of four signals.

^{1}H-NMR studies at high temperature were also performed for all the complexes. However, only the NMR spectra of **3**–**6** are temperature dependent. By increasing the temperature we observed for these complexes the broadening and coalescence of the resonances due to the tetrakis(pyrazoly)borate ligands. Finally, at 340 K (**3**,**6**) and at 360 K (**5**) spectra with only one set of three resonances were obtained, due to the H(3), H(4) and H(5) protons of the tetrakis(pyrazolyl)borate ligands (see Section 2). This result indicates that at these temperatures all the pyrazolyl rings became magnetically equivalent. This equivalence is explained by the existence of two dynamic processes: one is intramolecu-

Table 2
^{1}H-NMR data for complexes **1**–**8** at r.t.[a]

Complex	$[B(pz)_4]^-$						Other ligands
	Coordinated			Uncoordinated			
	H(3)	H(4)	H(5)	H(3)	H(4)	H(5)	
1	18.9 (6H)	7.0 (6H)	4.7 (6H)	5.8 (2H)	4.4 (2H)	2.8 (2H)	–
2	32.9 (6H)	6.8 (6H)	0.24 (6H)	3.2 (2H)	1.0 (2H)	−5.82 (2H)	187.9 (2H, CH_2) 71.4 (3H, CH_3)
3	28.4 (6H)	6.7 (6H)	1.1 (6H)	3.4 (2H)	1.9 (2H)	−6.05 (2H)	70.2 (9H, CH_3)
4	30.9 (6H)	6.5 (6H)	−0.6 (6H)	3.7 (2H)	1.2 (2H)	−4.47 (2H)	71.6 (1H, *o*-H), 35.8 (1H, *m*-H), 35.2 (1H, *m*-H), 25.9 (1H, *p*-H), 12.2 (3H, *o*-CH_3)
5	–	–	–	3.1 (2H)	1.4 (2H)	−3.5 (2H)	44.6 (3H, *o*-CH_3), 41.4 (1H, *m*-H), 38.4 (1H, *m*-H), 27.1 (3H, *o*-CH_3), 23.4 (3H, *p*-CH_3),
6	–	–	–	–	–	–	15.3 (18H, CH_3)
7	28.6 (6H)	7.0 (6H)	1.3 (6H)	4.0 (2H)	1.2 (2H)	−4.5 (2H)	16.7 (2H, C*H*(CH_3)$_2$), 13.3 (12H, CH(*C*H_3)$_2$)
8	29.3 (6H)	6.7 (6H)	0.87 (6H)	3.8 (2H)	1.7 (2H)	−3.9 (2H)	184.9 (3H, CH_3)

[a] All the spectra were run in toluene-d_8, except for **1** (CH_2Cl_2-d_2). The chemical shifts are in ppm; downfield shifts are positive.

lar and dissociative, promoting an exchange between coordinated and uncoordinated rings, and the other is the usual SAP⇔DD⇔BCTP interconversion. At those temperatures both processes are fast on the NMR time scale and this justifies the very simple pattern obtained. For **7** this equivalence was never observed, due to the thermal instability of the complex.

Due to the complexity of the spectra in the region of the tetrakis(pyrazolyl)borate we were not able to determine the activation energy for any of these two dynamic processes. However, in these studies we calculated for **5** the activation energy for the rotation of the OR group around the U–OR bond. As can be seen in Table 2, at r.t. two resonances for the *o*-Me groups and two for the *m*-H protons of the aryloxide ligand appear. By increasing the temperature, the two resonances assigned to the *o*-Me groups broaden and collapse. At 330 K only one signal was obtained for these two groups and appears at 37.0 ppm. The same type of behaviour was observed for the two resonances assigned to the *m*-H protons, which appear as one signal at 340 K (35.0 ppm). Using the behaviour of these resonances it was possible to calculate the activation energy for the rotation of the OR group, at the coalescence temperature [26]: $\Delta G^{\neq}_{Tc} = 77$ kJ mol^{-1} ($Tc = 335$ K, $\delta_{m\text{-H}} = 2.2 + 11.6 \times 10^3$ T^{-1}, $\delta_{m\text{-H}} = 1.6 + 11.0 \times 10^3$ T^{-1}; $(\Delta\delta)_{Tc} = (\delta_1 - \delta_2)_{Tc} = 211$ Hz). This value is higher than the value found for the same process in the complex [UCl(OC$_6$H$_2$-2,4,6-Me$_3$){HB(pz)$_3$}$_2$] ($\Delta G^{\neq}_{Tc} = 62$ kJ mol^{-1}). This difference certainly accounts for the presence of the uncoordinated pyrazolyl rings in **5**, which leads to a more congested complex [20].

3.2. Solid state and molecular structures

The ORTEP drawings of complexes **1**, **5** and **7** are shown in Figs. 1–3. Selected bond distances and angles are listed in Tables 3–5.

The structures consist of discrete molecules in which the uranium atom is eight-coordinated in a distorted square antiprismatic (**1** and **7**) and in a bicapped triangular prismatic (**5**) geometry (Figs. 4–6).

In complex **1** both 'square' faces, Cl(a)–N(1a)–N(2a)–N(3) and Cl–N(1)–N(2)–N(3a), are quite folded, with dihedral angles of 9.4 and 9.9°, respectively, which led the distortion of the SAP along the geometric pathway towards the dodecahedron (DD). For complex **7** the distortion of the SAP along the geometric pathway towards the dodecahedron (DD) is even more significant as the 'square' faces are more folded: dihedral angles of 15.8 and 17.3° for the faces N(3)–N(1a)–N(2a)–S and N(1)–N(3a)–S(a)–N(2), respectively. For **5** the rectangular face of the bicapped trigonal prism (BCTP), atoms Cl–N(2)–N(6)–N(7), is almost planar with a δ value of 0.6° and the δ value for the unique rectangular edge, O–N(3), is 32.1°, which are close to the δ values of 0.0 and 21.8° for the idealized BCTP. The triangular faces Cl–N(7)–O and N(3)–N(2)–N(6) are almost parallel (Table 6).

The distorted SAP⇔DD geometries found for **1** and **7** compare with the distorted geometries found in analogous complexes [UX$_2${HB(pz)$_3$}$_2$] (X = OC$_6$H$_4$-*o*-Me, S^{i}Pr) previously characterized [19,22]. The coordination geometry found for complex **5** is unusual for U(IV) and Th(IV) complexes and is only comparable to the eight-coordinate [Ce(acac){HB(pz)$_3$}$_2$] and [Yb{η^2-HB(pz)$_3$}{HB(pz)$_3$}$_2$] [27,28].

In complex **1** the U–Cl bond distance and the Cl–U–Cl bond angle are 2.609(5) Å and 86.0(2)°, respect-

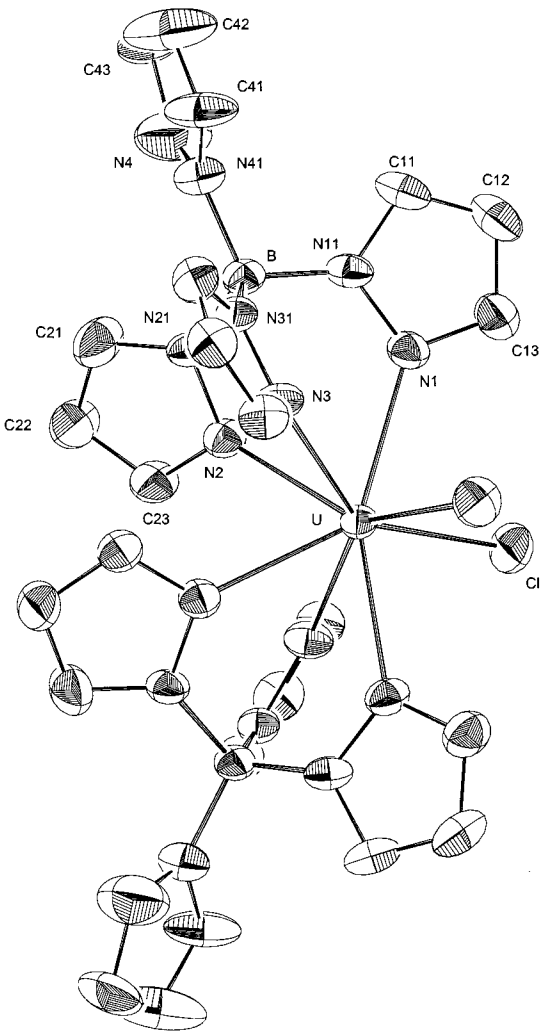

Fig. 1. ORTEP view of **1**.

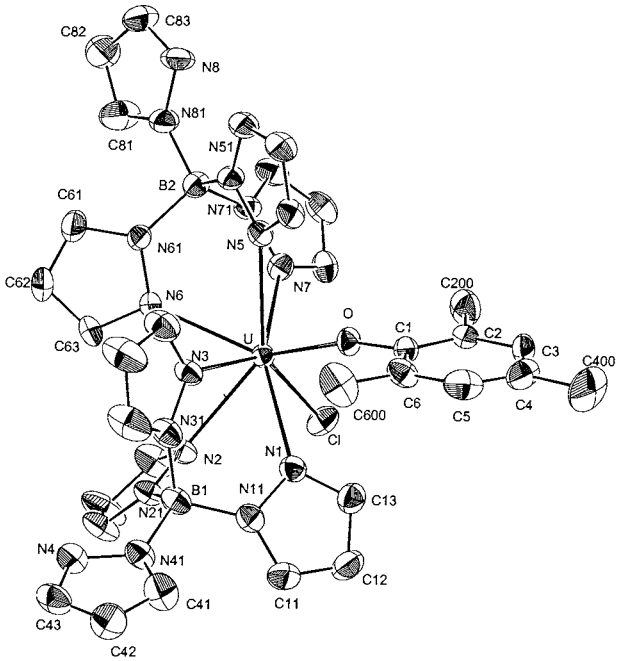

Fig. 2. ORTEP view of **5**.

ively. It is not very accurate to compare these values with the ones found for the analogous $[UCl_2\{HB(pz)_3\}_2]$, as the quality of the crystal was not very good, and we had two molecules per asymmetric unit for this complex. Taking into account the difference of 0.05 Å between the ionic radius of uranium and thorium, a comparison with the structure of $[ThCl_2\{HB(pz)_3\}_2]$ [25] shows similar An–Cl bond length (average 2.68 (**1**) Å) and Cl–Th–Cl angle (85.4(2)°). In complex **5** the U–Cl bond distance (2.662(2) Å) is larger than the corresponding bond distance in **1** (2.609(5) Å), but is comparable to the values found in other alkoxides with $HB(pz)_3$ ligands: $[UCl(OC_2H_5)\{HB(pz)_3\}_2]$ (2.690(5) Å), $[UCl(OC_6H_5)\{HB(pz)_3\}_2]$ (2.682(6) Å) and $[UCl(O^tBu)\{HB(pz)_3\}_2]$ (2.697(2) Å) [19–22]. Although the

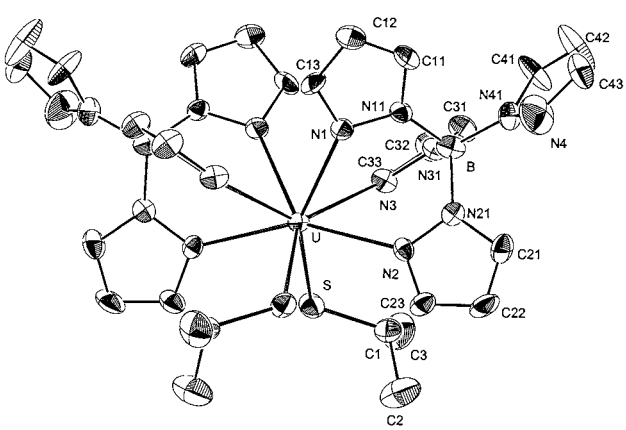

Fig. 3. ORTEP view of **7**.

Table 3
Selected bond lengths (Å) and bond angles (°) for $[UCl_2\{B(pz)_4\}_2]$ (**1**)

Bond lengths (Å)			
U–Cl	2.609(5)	B–N[b]	1.54(1)
U–N(1)	2.529(8)	N–N[b]	1.36(1)
U–N(2)	2.578(8)	C–N[b]	1.34(1)
U–N(3)	2.561(8)	C–C[b]	1.37(3)
Bond angles (°)			
B–U–B	126.5(2)	N(2)–U–N(1)	70.4(3)
Cl–U–Cl[a]	86.0(2)	N(3)–U–N(1)	69.5(3)
N(1)–U–Cl	77.5(2)	N(3)–U–N(2)	74.0(3)
N(2)–U–Cl	111.0(2)	N(1)–U–N(1)[a]	154.9(3)
N(3)–U–Cl	142.7(1)	N(1)–U–N(2)[a]	133.2(3)
N(1)–U–Cl[a]	84.1(2)	N(1)–U–N(3)[a]	120.4(3)
N(2)–U–Cl[a]	144.5(2)	N(2)–U–N(2)[a]	73.5(3)
N(3)–U–Cl[a]	71.1(2)	N(2)–U–N(3)[a]	72.8(3)
N–B–N[b]	109.5(6)	N(3)–U–N(3)[a]	138.2(3)

[a] The equivalent atoms were generated by the symmetry operation $-x, y, -z+1/2$.
[b] Mean value for the pyrazolyl rings.

replacement of a chloride by a bulky alkoxide could explain these differences, this is not so clear when we consider the ethoxide ligand. Steric reasons are not so evident in this case. A more general reason would be the existence of a strong π interaction between the uranium and oxygen atoms, normally reflected in short U–O bond distances and large U–O–R bond angles. In **5** evidence for this type of interaction is also present, as shown by the short U–O bond distance (2.081(4) Å) and by the large U–O–C bond angle (165.2(4)°) [29].

Table 4
Selected bond lengths (Å) and bond angles (°) for $[UCl(OC_6H_2\text{-}2,4,6Me_3)\{B(pz)_4\}_2]$ (**5**)

Bond lengths (Å)			
U–Cl	2.662(2)	U–O	2.081(4)
U–N(1)	2.592(5)	U–N(5)	2.620(5)
U–N(2)	2.571(5)	U–N(6)	2.558(5)
U–N(3)	2.507(5)	U–N(7)	2.593(5)
O–C(1)	1.373(7)		
B–N[a]	1.54(1)	C–C[a]	1.36(2)
C–N[a]	1.34(1)	C–C[b]	1.38(1)
N–N[a]	1.36(1)	C–CH_3[b]	1.51(1)
Bond angles (°)			
Cl–U–O	95.24(12)	N(2)–U–N(1)	67.0(2)
N(1)–U–Cl	78.26(12)	N(3)–U–N(1)	71.2(2)
N(2)–U–Cl	75.69(12)	N(3)–U–N(2)	73.1(2)
N(3)–U–Cl	142.81(12)	N(5)–U–N(6)	72.4(2)
N(5)–U–Cl	137.35(12)	N(5)–U–N(7)	68.3(2)
N(6)–U–Cl	114.47(13)	N(6)–U–N(7)	70.9(2)
N(7)–U–Cl	74.61(11)	N(1)–U–N(5)	130.9(2)
U–O–C(1)	165.2(4)	O–U–N(1)	71.9(2)
O–U–N(2)	138.8(2)	O–U–N(3)	95.0(2)
O–U–N(5)	72.2(2)	O–U–N(6)	144.3(2)
O–U–N(7)	100.5(2)	N–B–N[a]	110(2)
B–U–B	129.2(2)		

[a] Mean value for the pyrazolyl rings.
[b] Mean value for the aromatic ring.

Table 5
Selected bond lengths (Å) and bond angles (°) for $[U(S^iPr)_2\{B(pz)_4\}_2]$ (**7**)

Bond lengths (Å)			
U–S	2.683(3)	S–C(1)	1.819(12)
U–N(1)	2.550(8)	C(1)–C(2)	1.51(2)
U–N(2)	2.584(9)	C(1)–C(3)	1.53(2)
U–N(3)	2.604(9)	C–C[a]	1.36(3)
B–N[a]	1.54(2)	C–N[a]	1.34(2)
N–N[a]	1.36(1)	N–B–N[a]	110(1)
Bond angles (°)			
S–U–S[b]	93.67(14)	N(2)–U–N(1)	71.4(3)
U–S–C(1)	116.5(4)	N(3)–U–N(1)	72.6(3)
N(1)–U–S	146.8(2)	N(3)–U–N(2)	67.9(3)
N(2)–U–S	89.9(2)	N(1)–U–N(1)[b]	71.7(4)
N(3)–U–S	75.0(2)	N(1)–U–N(2)[b]	132.7(4)
N(1)–U–S[b]	105.8(2)	N(1)–U–N(3)[b]	73.5(3)
N(2)–U–S[b]	72.5(2)	N(2)–U–N(2)[b]	154.4(4)
N(3)–U–S[b]	138.6(2)	N(2)–U–N(3)[b]	122.4(4)
B–U–B	126.8(2)	N(3)–U–N(3)[b]	137.8(4)

[a] Mean value for the pyrazolyl rings.
[b] The equivalent atoms were generated by the symmetry operation $-x, y, -z+1/2$.

In complex **1** the U–N bond distances range from 2.529(8) to 2.578(8) Å with a mean value of 2.56(2) Å which is comparable to the values found in the uranium complexes $[UCl_2\{HB(pz)_3\}_2]$ (average 2.55(2) Å), $[UCl(O^tBu)\{HB(pz)_3\}_2]$ (2.60(3) Å) and $[UCl(OC_6H_5)\{HB(pz)_3\}_2]$ (2.57(2) Å). These values also compare with the U–N bond distances found in **5** (average 2.57(4) Å, range 2.507(5)–2.620(5) Å) and in **7** (average 2.58(2) Å, range 2.550(8)–2.604(9) Å).

In **5** the bond angle O–U–Cl (95.2(1)°) is larger than the corresponding values in the analogous $[UCl(OC_6H_5)\{HB(pz)_3\}_2]$ (86.2(5)°), $[UCl(O^tBu)\{HB(pz)_3\}_2]$ (87.4(2)°) and $[UCl(OC_2H_5)\{HB(pz)_3\}_2]$ (87.9(3)°). It is clear that the replacement of a chloride atom by an alkoxide increases the X–U–X bond angle but the found values do not seem to be directly related with the uncoordinated pyrazolyl rings or with the volume of the alkoxide. However, the above mentioned π interactions can lead to a widening of this angle as predicted by EHMO calculations (vide infra).

For complex **7** the U–S bond distance and the S–U–S bond angle are 2.683(3) Å and 93.67(14)°, respectively. These values are smaller than the corresponding values found for the eight-coordinate complex $[Th(S^nPr)_2\{C_5Me_5\}_2]$ (2.718(3) Å and 102.5(3)°) [30]. These differences are certainly due to the larger ionic radius of Th compared to U and also due to size and form of the pentamethylcyclopentadienyl compared to the poly(pyrazolyl)borate ligand [31]. Relatively to the analogous $[U(S^iPr)_2\{HB(pz)_3\}_2]$, the U–S bond dis-

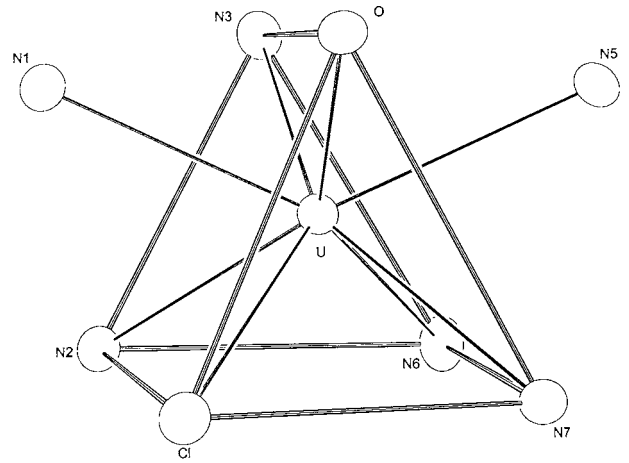

Fig. 5. Coordination polyhedron of **5**.

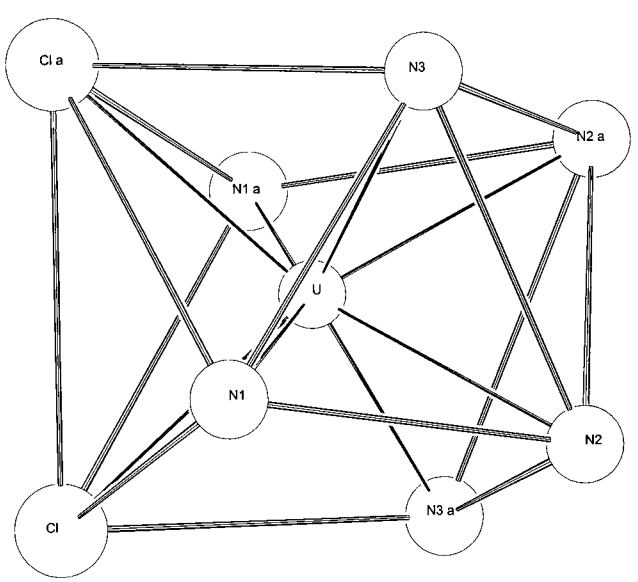

Fig. 4. Coordination polyhedron of **1**.

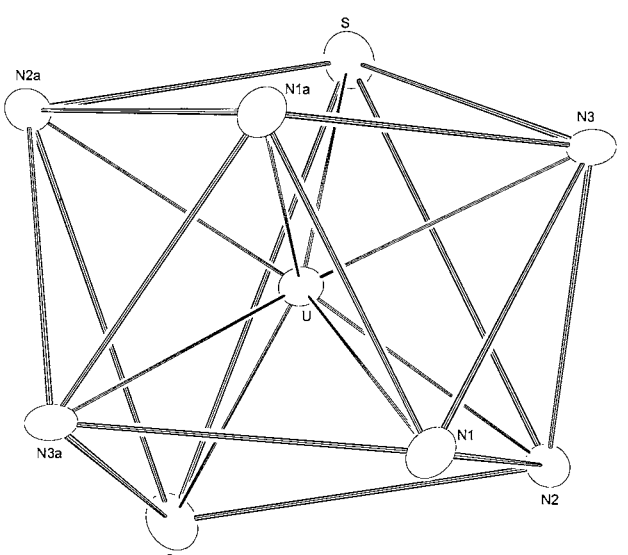

Fig. 6. Coordination polyhedron of **7**.

Table 6
Values of the δ and ϕ shape parameters (°) for $[UCl(OC_6H_2\text{-}2,4,6Me_3)\{B(pz)_4\}_2]$[a]

		p	np	SAP	BCTP	DD
δ_s	Cl [N(2) N(7)] N(6)	1.3	0.6	0.0	0.0	29.5
δ_s	N(1) [O N(3)] N(5)	21.4	32.1	0.0	21.8	29.5
δ_l	N(1) [N(2) N(3)] N(6)	45.5	46.7	52.5	48.2	29.5
δ_l	Cl [O N(7)] N(5)	27.1	35.1	52.5	48.2	29.5
ϕ	N(3)–N(1)–Cl–N(7)	16.4	16.4	24.5	14.1	0.0
ϕ	O–N(5)–N(6)–N(2)	7.7	6.6	24.5	14.1	0.0

[a] p, polyhedron; np, normalized polyhedron; δ_s, dihedral angles referred to the diagonals of the square faces of the polyhedron; δ_l, dihedral angles referred to the lateral edges of the polyhedron; ϕ, values for the planarity of the two orthogonal trapezoids.

tance is comparable (2.680(6) Å), but the S–U–S bond angle found for **7** is smaller than the corresponding bond angle in $[U(S^iPr)_2\{HB(pz)_3\}_2]$ (96.4(5)°). This difference may certainly be due to the presence of the uncoordinated pyrazolyl rings, which limits the bite of the ligand.

3.3. Molecular orbital calculations

Our experience with the chemistry of U(IV) reveals that the sterically less congested dichlorocomplexes with $\{HB(pz)_3\}$ and $\{B(pz)_4\}$ ligands can be prepared, namely $[UCl_2\{HB(pz)_3\}_2]$ and $[UCl_2\{B(pz)_4\}_2]$ (**1**). X-ray structural analysis showed for these complexes identical coordination numbers and identical solid structures with minor differences in angles and bonds. In solution both compounds are fluxional and an intramolecular non-dissociative process seems to explain the simple ^{1}H-NMR spectra obtained at r.t. However, we found differences in the derivative chemistry, especially with alkyls and with bulky oxygen, sulfur and nitrogen donors coligands. We found that it was possible to prepare a larger number of derivatives using $[UCl_2\{HB(pz)_3\}_2]$ as a precursor rather than using $[UCl_2\{B(pz)_4\}_2]$ (**1**) [19–25]. We performed molecular orbital calculations of the extended Hückel type (EHMO) to get a better insight into the differences found in the stability and structural trends of the U(IV) complexes with the ligands in a tripodal conformation.

Since the intraligand contact interactions between pyrazolyl rings bonded to the boron atom may condition the coordination geometry of the ligand, namely its bite, we performed an optimisation of the relevant parameters of the free ligand: most of the parameters are mutually dependent and we have chosen the B–N–N′ bond angle and N′···N′ bond distance (bite) as the independent ones, Fig. 7(a).

For the ligand shown in Fig. 7(a), with a fourth pyrazolyl ring, an aditional optimisation of the N#–N*–B–N torsion angle is necessary. The Walsh diagram (Fig. 7(b)) shows that the axial ring is always nearly planar with one of the tripodal pyrazolyl rings, bringing the two nitrogen atoms N# and N *trans* to each other. The Walsh diagram also shows that the HOMO orbital follows the behaviour of the energy plot

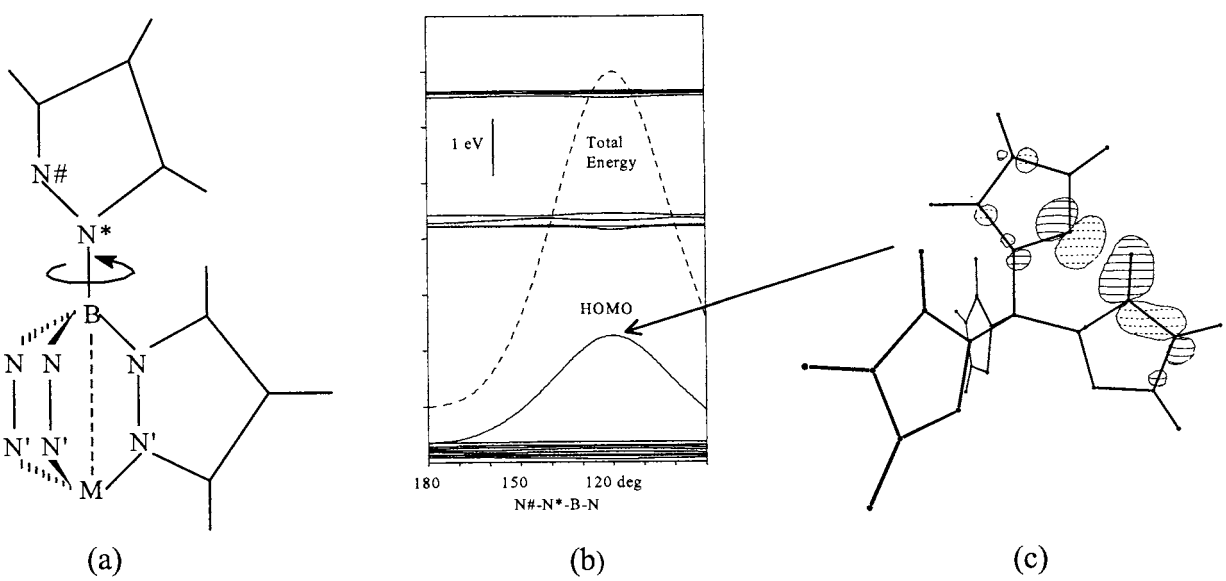

Fig. 7. Walsh diagram for the rotation of the axial pyrazolyl ring.

being responsible for this trend. A drawing of this orbital at the most unfavorable conformation (Fig. 7(c)) shows an anti-bonding interaction between the $N^{\#}$ lone pair and the hydrogen 1s orbital which disappears when the two hydrogens are pointing to each other. This feature was used to help in the assignment of the different Fourier peaks in the X-ray refinement of the 5-membered pyrazolyl rings and to define which peak was a nitrogen and which one was a carbon atom.

From the two independent structural parameters chosen to define the geometry of the poly(pyrazolyl) ligand, the B–N–N′ angle and the bite, we first optimized the B–N–N′ angle for a fixed bite of 2.85 Å. The EHMO calculations showed that a very soft minimum occurs around 119°. To simplify our model, a value of 120° was used through out all the calculations.

The first step in our calculations was to predict, for each of the free ligands [$HB(pz)_3$] and [$B(pz)_4$], the most favourable bite. The Walsh diagrams, Fig. 8, show that the most favourable bites are 3.05 Å for R = H and 2.85 Å for R = pz.

The ideal bite results from a balance between the repulsive interactions of the nitrogen lone pairs, HOMO orbital (Fig. 9(a)), which favours larger bites, and the attractive interactions of the same lone pairs (Fig. 9(b)) favouring shorter bites.

When R = pz in $RB(pz)_3$ and for larger bites, an extra anti-bonding interaction between adjacent hydrogens appears (Fig. 10) reducing the ideal bite by 0.2 Å.

When interacting these ligands with a metallic fragment—uranium in our work—we found that the maximum overlap population is achieved at a bite of 3.05 Å for both ligands. This value, as seen before, is the ideal bite for $HB(pz)_3$, but for $B(pz)_4$ this bite is energetically unfavorable due to repulsive interactions between *ortho* hydrogens of the pyrazolyl rings, which are in the same plane. This feature on its own makes all complexes with $B(pz)_4$ more unstable that their $HB(pz)_3$ counterparts.

Since all the complexes studied in this work have two stabilizing poly(pyrazolyl) ligands we decided to study the energetic behaviour and structural trends of the UL_2 fragment (L = $HB(pz)_3$ and $B(pz)_4$). The analysis of the frontier orbitals did not show any significant differences between the two analysed ligands, both similar to our previously reported work [19]. The structural trend of the L–U–L angle, Fig. 11, has a similar behaviour for both ligands, accepting L–U–L angles above 124° without major energetic unstabilization. This value is in the low end of the experimental range observed for this family of complexes, 124.7–131.1° [3,19]. All subsequent calculations were done with an angle of 124°, since it is the most favourable for the introduction of two extra ligands in a pseudo tetrahedric geometry.

Previous results [19] showed that in a pseudo tetrahedral environment the fragment UL_2^{2+} has three empty frontier orbitals, located in the bisecting L–U–L plane, Fig. 12, that can interact with extra ligands to form complexes of the type [$UXZL_2$].

The **1a**,**b** orbitals have appropriate symmetry to make σ interactions with two ligands, X and Z, located at the bisecting L–U–L plane, while the **2a** can be involved in π interactions. In this way σ-donors will have a tendency to adopt smaller X–U–Z angles to maximize the overlap population with orbitals **1a** and **b**, while π-donors will maximize this parameter at wider angles due to the competing π-interaction with the **2a** orbital. In our complexes this widening will be limited by stereochemical interactions with the pyrazolyl rings of the stabilizing $RB(pz)_3$ ligands.

When the two extra ligands X and Z are chlorine atoms, [UCl_2L_2], the optimized Cl–U–Cl angle is 76° with a flat minima in the range 72–84° (Fig. 13). No significant differences are observed for R = H or pz in $RB(pz)_3$.

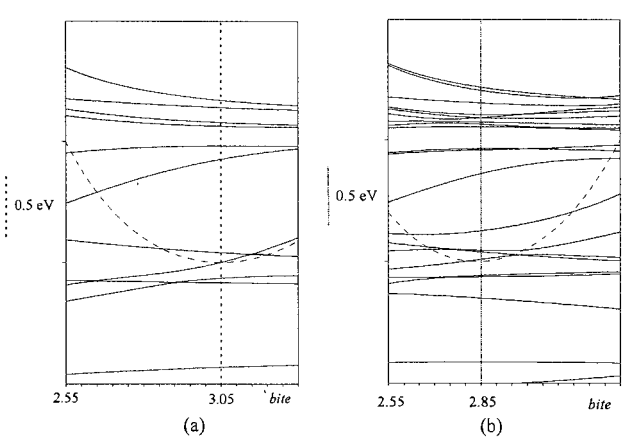

Fig. 8. Walsh diagrams for the free ligands: (a) [$HB(pz)_3$] and (b) [$B(pz)_4$]. Only the occupied orbitals are shown.

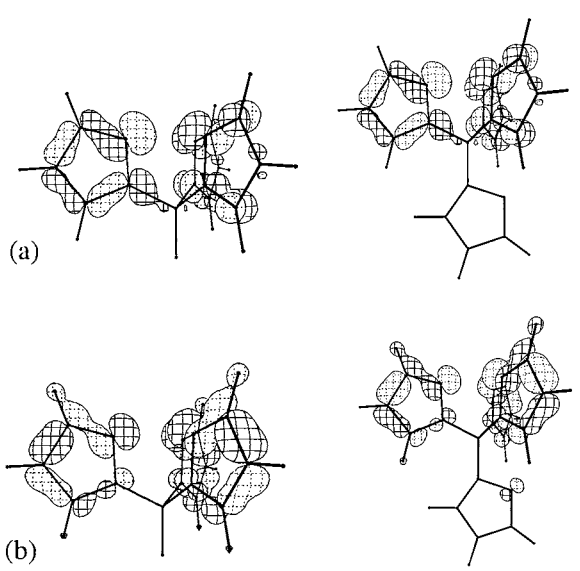

Fig. 9. (a) HOMO orbitals of [$HB(pz)_3$] and [$B(pz)_4$]; (b) C_3 symmetric combination of nitrogen lone pairs of [$HB(pz)_3$] and [$B(pz)_4$].

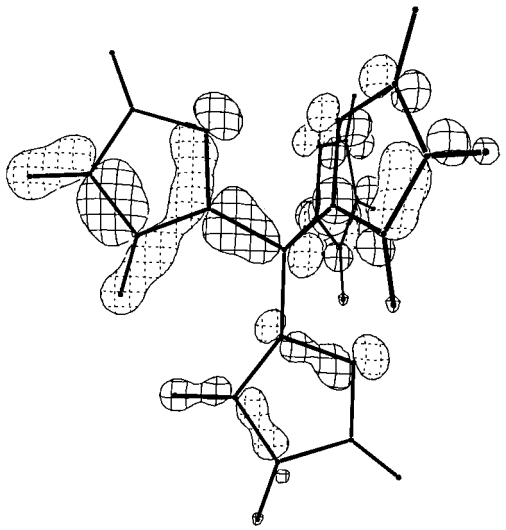

Fig. 10. Repulsive interactions between 1s orbitals of *ortho* hydrogens of $[B(pz)_4]$.

Replacing one chlorine by a methyl group the observed trend does not change, being the optimized Cl–U–Me angle 72°. These X–U–Z angles are all smaller than the experimental ones (84.1–96.4°) [3,19], as we forced the L–U–L angle at the lower end of the possible range. More bulky alkyl ligands, like the attempted benzyl, require the optimizition of the 6 membered ring conformations defined by the torsion angles Cl–U–C–C and U–C–C–C. For $HB(pz)_3$ the benzyl ligand is almost coplanar with the Cl atom (Cl–U–C–C = 15°), but the 6-membered ring is twisted by 60° (U–C–C–C). At this optimum conformation the Cl–U–C angle widened to 92°. A major difference is observed when the stabilizing ligand is $B(pz)_4$, because there is not enough room to fit the benzylic hydrogens in near planar conformations of the benzyl ligand. Strong repulsive interactions between the hydrogens of the benzyl and of the pyrazolyl prevent torsions of the benzyl below 45° (Cl–U–C–C = 45° and U–C–C–C = 75°). The Cl–U–C angle is also at 92°. Even at this energy minimum the interaction between the fragment UL_2^{2+} and the chloride and benzyl ligands is anti-bonding by 0.8 eV for (Bpz_4) and slightly bonding (0.4 eV) for $HBpz_3$. Since the stereochemical interactions between benzyl and $HB(pz)_3$ are on the edge of allowing

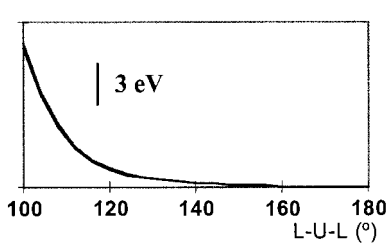

Fig. 11. Energetic trends of L–U–L angle, L = $[HB(pz)_3]$ or $[B(pz)_4]$.

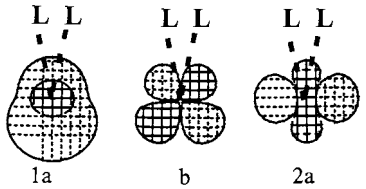

Fig. 12. Frontier orbitals of UL_2^{2+}.

the stabilization of such compounds, replacing the chloride co-ligand by a stronger donor ligand like OEt, allowed us to prepare the benzyl derivatives, as described in our previous work [19], while all the attempts made with $B(pz)_4$ failed.

When one oxygen donor ligand containing bulky R groups is present the stereochemical interactions between the pyrazolyl rings and the aryloxide are less severe due to the large U–O–C bond angle (170°). With thiolates the increase of the U–S bond length, 2.68 Å, when compared with the uranium oxygen bond length, 2.08 Å, enables the ligand to adopt a more favourable U–S–C angle of 120° without major interactions with $B(pz)_4$. In fact, this seems to explain the possibility of synthesizing aryloxides and thiolate derivatives with $HB(pz)_3$ and $B(pz)_4$ ligands, and the limitations found for alkyl derivatives in the system with $B(pz)_4$ ligands.

3.4. Concluding remarks

We have shown that $[UCl_2\{B(pz)_4\}_2]$ (**1**) does not present significant differences relative to the analogous $[UCl_2\{HB(pz)_3\}_2]$ in which concerns the solid state structure and solution behaviour. However, the derivative chemistry of **1** is much more limited, especially when alkyl groups other than methyl are involved. Complexes **1**–**8** are fluxional in solution and two dynamic intramolecular processes seem to be involved: one is dissociatve and another nondissociative. The analysis of the frontier orbitals did not show any significant differences for the $HB(pz)_3$ and $B(pz)_4$ ligands. However, the calculations seem to indicate that stereochem-

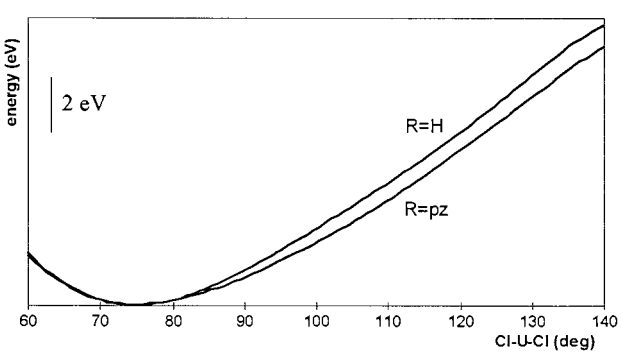

Fig. 13. Energy plot for the optimization of the Cl–U–Cl angle in UL_2Cl_2.

Table 7
Exponents and parameters for uranium

Orbital	$-H_{ii}$ (eV)	ξ_1	ξ_2	C_1	C_2
U 7s	5.5	1.914			
U 7p	5.5	1.914			
U 6p	30.03	4.033			
U 6d	9.19	2.581	1.207	0.7608	0.4126
U 5f	10.62	4.943	2.106	0.7844	0.3908

ical interactions condition the reactivity of complexes stabilized by different poly(pyrazolyl)borates, by imposing unfavourable coordination geometries.

Acknowledgements

M.P.C. Campello gratefully acknowledges PRAXIS XXI for a PhD grant.

Appendix A

All the calculations were of the extended Hückel [32] type with modified H_{ij}'s [33]. The basis set for the metal atoms consisted of ns, np, (n-1)p, (n-1)d and (n-2)f orbitals. The s and p orbitals were described by single Slater type wave functions, and d and f orbitals were taken as contracted linear combinations of two Slater type wave functions. Only s and p orbitals were used for Cl, S, C, O, N.

Standard parameters were used for C, H, N, Cl and S, while those for the uranium atom were obtained by using a semirelativistic approach (Table 7, [34]).

The structural parameters were taken from the crystal structures presented in this work.

References

[1] S. Trofimenko, Chem. Rev. 93 (1993) 943.
[2] N. Kitajima, W.B. Tolman, Prog. Inorg. Chem. 43 (1995) 419.
[3] I. Santos, N. Marques, New J. Chem. 19 (1995) 551.
[4] (a) S. Trofimenko, J. Am. Chem Soc. 88 (1966) 1842. (b) S. Trofimenko, J. Am. Chem. Soc. 89 (1967) 3170.
[5] Y. Sohrin, H. Kokusen, S. Kihara, M. Matsui, Y. Yushi, M. Shiro, J. Am. Chem Soc. 115 (1993) 4128.
[6] Y. Sohrin, M. Matsui, Y. Hata, H. Hasegawa, H. Kokusen, Inorg. Chem. 33 (1994) 4376.
[7] D.D. Perrin, W.L.F. Armarego, Purification of Laboratory Chemicals, 3rd Edn, Pergamon Press, Oxford, 1988.
[8] J.A. Hermann, J.F. Suttle, Inorg. Synth. 5 (1957) 143.
[9] M.R. Collier, M.F. Lappert, R. Pearce, J. Chem. Soc. Dalton Trans. (1973) 445.
[10] J.F. Eastham, C.G.U.S. Screttas, Patent 3534113, Chem Abstr. 74 (1971) 3723b.
[11] L.E. Manzer, J. Organomet. Chem. C6 (1977) 135.
[12] C.K. Fair, MOLEN, Enraf–Nonius, Delft, The Netherlands, 1990.
[13] G.M. Sheldrick, SHELXS-86: Program for Solution of Crystal Structure, University of Göttingen, Germany, 1986.
[14] (a) G.M. Sheldrick, SHELX: Crystallographic Calculation Program, University of Cambridge, UK, 1976. (b) G.M. Sheldrick, SHELXL-93: Program for Crystal Structure Refinement, University of Göttingen, Germany, 1993.
[15] J.A. Ibers, W.C. Hamilton, International Tables of X-ray Crystallography, vol. IV, Kynoch Press, Birmingham, 1973.
[16] C.K. Johnson, ORTEPII: Report ORNL-5138, Oak Ridge, National Laboratory, Oak Ridge, TN, 1976.
[17] K.W. Bagnall, A.C. Tempest, J. Takats, A.P. Masino, Inorg. Nucl. Chem. Lett. 12 (1976) 555.
[18] (a) D. Cohen, T.W. Carnall, J. Phys. Chem. 64 (1960) 1933. (b) D.C. Moody, J.D. Odom, J. Inorg. Nucl. Chem. 4 (1979) 533. (c) P. Zanella, G. Rossetto, G. De Paoli, O. Traverso, Inorg. Chim. Acta 44 (1980) L155. (d) J.E. Nelson, D.L. Clark, C.J. Burns, A.P. Sattelberger, Inorg. Chem. 31 (1992) 1973. (e) M.A Carvalho, A. Domingos, P. Gaspar, N. Marques, A. Pires de Matos, I. Santos, Polyhedron 11 (1992) 1481. (f) J.E. Nelson, D.L. Clark, L.R. Avens, S.G. Bott, D.L. Clark, A.P. Sattelberger, J.G. Watkin, B.D. Zwick, Inorg. Chem. 33 (1994) 2248.
[19] M. Paula, C. Campello, M.J. Calhorda, A. Domingos, A. Galvão, J.P. Leal, A. Pires de Matos, I. Santos, J. Organomet. Chem. 538 (1997) 223.
[20] I. Santos, J. Marçalo, N. Marques, A. Pires de Matos, Inorg. Chim. Acta 134 (1987) 315.
[21] A. Domingos, A. Pires de Matos, I. Santos, J. Less Common Met. 148 (1989) 279.
[22] A. Domingos, A. Pires de Matos, I. Santos, Polyhedron 11 (1992) 1601.
[23] I. Santos, A. Pires de Matos, Actinides-89, Tashkent, URSS, 1989.
[24] M. Paula, C. Campello, A. Domingos, I. Santos, J. Organomet. Chem. 484 (1994) 37.
[25] A. Domingos, J. Marçalo, I. Santos, A. Pires de Matos, Polyhedron 9 (1990) 1645.
[26] J. Sandstron, Dynamic NMR Spectroscopy, Academic Press, New York, 1982.
[27] (a) M.A.J. Moss, C.J. Jones, A.J. Edwards, Polyhedron 7 (1988) 79. (b) M.A.J. Moss, C.J. Jones, A.J. Edwards, J. Chem. Soc. Dalton Trans. 1393 (1989).
[28] M.V.R. Stainer, J. Takats, Inorg. Chem. 21 (1982) 4050.
[29] C. Baudin, D. Baudry, M. Ephritikhine, M. Lance, A. Navaza, M. Nierlich, J. Vigner, J. Organomet. Chem. 415 (1991) 59.
[30] Z. Lin, C.P. Brocke, T.J. Marks, Inorg. Chim. Acta 144 (1988) 145.
[31] J. Marçalo, A. Pires de Matos, Polyhedron 20 (1989) 2431.
[32] R. Hoffmann, J. Chem. Phys. 39 (1963) 1397.
[33] J.H. Ammeter, H.-B. Bürgi, J.C. Thibeault, R. Hoffmann, J. Am. Chem. Soc. 100 (1978) 3686.
[34] K. Tatsumi, A. Nakamura, J. Am. Chem. Soc. 109 (1987) 3195.